INTERNATIONAL JOURNAL OF RESEARCH CULTURE SOCIETY ISSN: 2456-6683 Volume - 4, Issue - 7, July – 2020
Monthly, Peer-Reviewed, Refereed, Indexed Journal Scientific Journal Impact Factor: 5.743
Received on : 26/06/2020 Accepted on : 14/07/2020 Publication Date: 31/07/2020

Adsorption behaviour of Arsenic (V) by cellulose /magnetic chitosan composite

[1] K. Jayaraj, [2] Jackcina Stobel Christy , [3] Anitha Pius*
Department of Chemistry, The Gandhigram Rural Institute- Deemed to be University
Gandhigram, Dindigul – 624 302, Tamil Nadu, India
Email - *dranithapius@gmail.com

Abstract: *The presentation of an anion exchanger (AE) arranged on coconut coir fiber which acts like a reinforcer in magnetic chtosan matrix, for the adsorption of arsenic (V) [As(V)] from aqueous solutions was assessed in this examination. The adsorbent (PCC–AENF) possessing dimethyl amino hydroxypropyl was prepared by the reaction of PCC with epichlorohydrin and dimethylamine followed by treatment of hydrochloric acid. IR spectroscopy results affirm the nearness of – NH + (CH3) $_2$Cl - group in the adsorbent. XRD studies affirm the presence of PCC–AENF. Batch tests were led to look at the proficiency of the adsorbent on As(V) expulsion. Most extreme adsorption of 99.2% was gotten for an underlying grouping of 1 mg l - 1As(V) at pH 7.0 and an adsorbent portion of 2 mg l $^{-1}$. The energy of sorption of As(V) onto PCC–AENF was depicted utilizing the pseudo-second-order model. The equilibrium isotherms were resolved for various temperatures and the outcomes were investigated utilizing the Langmuir condition. The temperature reliance demonstrates an exothermic procedure. Recovery studies were performed utilizing 0.1 N HCl. Batch adsorption–desorption considers represent that PCC–AENF in magnetic chitosan matrix could be utilized to expel As(V) from ground water and other modern effluents.*

Key Words: *Purified coir cellulose, magnetic chitosan, arsenic (V),*

Highlights

- Modified cellulose nanofibrils with high quaternary amines were achieved
- As(V) removal was rapid and the pseudo second order model best fitted the data
- The adsorption isotherms of As (V) removal were better described by the Langmuir model
- The Langmuir maximum capacity of modified cellulose nanofibrils was 25.5 mg g−1
- As V) adsorption onto modified cellulose nanofibrils is spontaneous

1. INTRODUCTION:

Arsenic is viewed as one of the most lethal heavy metals and it has been delegated a Group 1 human cancer-causing agent by the International Agency for Research on Cancer (IARC)(**1**) Arsenic is the twentieth most rich component in the Earth's crust, the fourteenth in seawater and the twelfth most copious component in the human body(**2**). There are two types of arsenic, to be specific arsenite [As (III)] and arsenate [As (V)]. Groundwater frameworks contain inorganic arsenic species as arsenite [As (III)] with an oxidation condition of +3 and arsenate [As (V)] with an oxidation condition of +5 (**3**). Ordinarily, As (V) exists as $H_2AsO_4^-$, $H_2AsO_4^{2-}$, and $AsO_4$3-in groundwater under oxidizing conditions inside pH range of 2 to 12. In the mean time, As (III) as H_3AsO_3 prevails under reducing, anaerobic conditions inside a pH range of 2 to 9 (**4**). When all is said in done, arsenic is found in trace amounts in both surface water and groundwater, however in higher fixation levels in groundwater.

Arsenic can discharge into the aquatic conditions by common procedures, for example, disintegration of minerals by weathering, microbial action, and complexation with organic materials (**5,6**) On the other hand, anthropogenic exercises, including modern mining and metallurgical enterprises, burning of petroleum products, utilization of arsenic pesticides, herbicides, and yield desiccants, can bring about arsenic defilement in soils and surface water(**7,8**). Arsenic contamination in groundwater at raised fixations is all around reported in numerous nations, for example, America, Argentina, Bangladesh, Chile, China, India and Mexico at a focus extend from 1 mg L^{-1} to 73.6 mg L^{-1}.(**9**). Persistent presentation to arsenic contamination cause harm to the central nervous system, kidney, skin, liver and lungs in people (**10**), mitochondrial superoxide dismutase (MSOD) exercises in liver and lungs, cause cardiovascular ailments, hypertension and influences vascular system(**11**). In human beings, long term contact with arsenic polluted water can prompt various skin diseases (**12**). Adsorption onto materials is viewed as the primary removal step of arsenic polluted substances. It is an alluring innovation because of its cost-adequacy, simple activity

and low maintanance. Also, it is applicable in family unit module and mechanical plants and has the limit with regards to adsorbent recovery (**13, 14**). In such manner, the quantity of ordinary adsorbents of natural and synthetic source, for example, sand, fly debris, plant biomass, activated carbon and alumina have been utilized to treat arsenic from groundwater (**15,16**).It is important to have a positive charge on the outside of the adsorbent to pull in anions like arsenate. Hence, surface alteration is the best way and it came into the spotlight for development in adsorption proficiency.

Cellulose is viewed as one of the most moderate and plentiful common crude materials accessible for the production of different useful materials (**17,18**). The rich hydroxyl groups on the cellulose can be utilized straightforwardly or adjusted with other functional groups to extricate poisonous metal particles from water. Lately, there is a developing enthusiasm for the use of characteristic lignocellulose materials as modest and eco-friendly adsorbents(**19**). Altered cellulose-based materials have been used in different natural applications including the removal of heavy metals, dyes and microorganisms (**20- 24**).

Various changes, for example, substance adjustment, have been utilized for improving physical and compound properties of the lignocellulose materials and to expand the adsorption limit like copolymerization, cross connecting and quaternisation (**25**). The current work is given to the readiness of an anion exchanger utilizing purified coir cellulose from coconut coir fiber, by its reaction with epichlorohydrin and dimethylamine followed by treatment with hydrochloric acid. This is then blended in with magnetic chitosan which has a strong take-up limit of arsenic species from aqueous mediums (**26**). In particular, the prepared composite material was characterised by different techniques. Further, the removal efficiency of this composite was assessed by considering the parameters like dosage, time, concentration, pH, and temperature. And after all, utilizing experimental information, a model was created to figure the removal efficiency.

2. MATERIAL AND METHODS:

2.1 Materials

All the chemicals used in this study were of analytical grade. A 1000 mg l_1 As(V) stock solution was prepared by dissolving a weighed quantity of Na_2HAsO_4 . 7H $_2$O (Aldrich, USA) in distilled water. All solutions for adsorption and analysis were prepared by appropriate dilution of the freshly prepared stock solution. Epichlorohydrin (Fluka, Switzerland) was used as received. Pyridine, dimethylformamide (DMF),dimethylamine, were obtained from M/S E.Merck, India. Low molecular weight chitosan, $FeCl_3.6H_2O$ and $FeSO_4.7H_2O$ were of analytical grade and purchased from Sigma–Aldrich.

2.2 Extraction and purification of cellulose

Then the coir fibers were Wiley-milled to 40–60 mesh (0.245–0.350 mm) and extracted with benzene-ethanol (v/v=2:1) in a Soxhlet extractor for 24 h to fully remove the extractives.The extractive-free sample was sonicated in a mixed aqueous solution for 30 min, which consisted of 0.5M NaOH and 0.5M CH3OH (v/v=2:1) (**27**) . The suspension was heated up and kept at 60 °C for 2.5 h under stirring. After that, the residue (crude coir cellulose product) was washed with deionized water until pH neutral. Repeat ii) and iii) once to further minimize the lignin content of the sample. The crude coir cellulose sample was charged into a mixed solution containing 5 wt% NaClO2 aqueous solution and CH3COOH (v/v=1:1) with a total solid-liquid ratio of 1:15 (g:mL), and the mixture was continually stirred and heated at 80 °C for 2 h. The entire bleaching step was repeated for twice. The final purified coir cellulose (PCC) was thoroughly rinsed with deionized water, lyophilized and kept in a desiccator for future use.

2.3 Surface modification of PCC to PCC- AE

The sensitive part used for cross linking is the hydrxylgroup of the cellulose. Scheme 1 presents the general method for the preparation of adsorbent. Amino groups were introduced into the epoxy propyl by-product after reaction with 100 ml of 50% dimethylamine solution for around 3 h maintaining the temperature in the range of 70–80 ^{0}C. To convert into an anion exchanger (AE), the above product was treated with 500 ml of 0.2 M HCl for 4 h at room temperature, washed well to remove excess chloride ions and dried at 80 ^{0}C. The functionalized PCC (PCC–AE) was sieved and particles having the average diameter of 0.096 mm were used throughout the study.

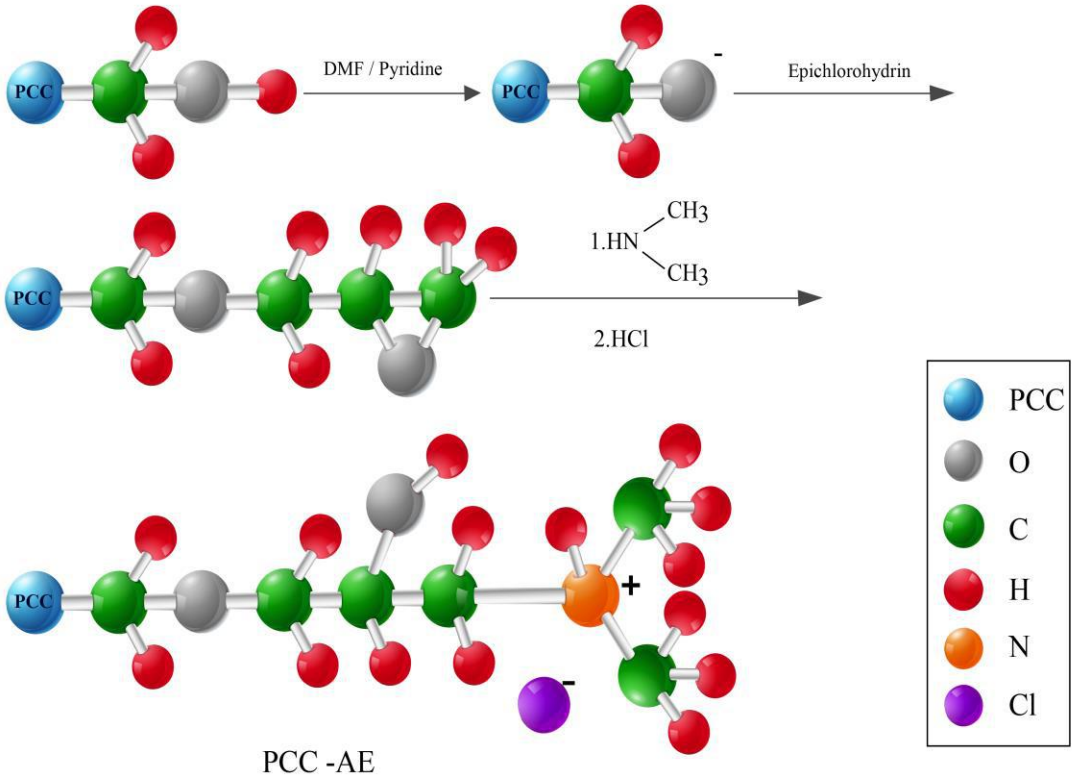

Scheme1. Preparation of PCC–AE

2.4. Preparation of coir cellulose nanofibrils (PCC- AENF)

0.2 g PCC-AE was dispersed into 50 ml deionized water and cooled up to 4 °C. The slurry was ultrasonicated for 1h. The suspension was centrifuged for 20 min to remove the unfribrillated parts. The final nanofibril suspension was stored at 4 °C for later use.

2.5. Preparation of PCC- AENF/ magnetic chitosan (MCHI) composite

3 g of chitosan was dissolved in 100 mL acetic acid (3%, v/v) at room temperature for 12 h. 4.20 g of FeCl2·4H2O and 11.42 g of FeCl3·6H2O were dissolved into 50 mL of deoxygenated distilled water. After stirring for 30 min, precipitation was observed under vigorous stirring by adding 45 mL of NH3·H2O solution (28%, v/v), followed by a further stirring for 2 h. The precipitates were separated and washed with ethanol and distilled water. Then, it was stirred at 60 ^{0}C for 30 min. Fe (III) (as FeCl3) and Fe (II) (as FeSO4) (0.02 mol: 0.01 mol) was dissolved and added into the above the mixed solution to obtain magnetic chitosan (**28**).The CCNF were added to the1 Wt% magnetic chitosan solution, in 9:1 ratios and the total concentration of mix was 2 wt%. The mixture was allowed to solidify and sieved in a mortar.

2.6 Characterisation

The FTIR spectra of PCC and PCC-AENF were obtained using the pressed disk technique on a Schimadzu FTIR model 1801. The XRD patterns of the adsorbent samples were obtained with a Siemens D 5005 X-ray unit using Ni-filtered Cu Ka radiation. A systronic microprocessor pH meter (model, l362, India) was used to measure the potential and pH of the suspension. Based on the standard method, an atomic absorption spectrophotometer, AAS (A 5450, GBC, Australia) equipped with a manual hydride generator (APU-49, Analytical Spectral Utilities, Hyderabad, India) was employed to determine the As concentration in solutions (**29**). For complete reduction of As(V), 5% KI and 10% ascorbic acid solutions were reacted with the samples. Following this procedure.After that, the sample was reacted with 3% NaBH4 and 1.5% HCl solutions. All measurements were based on absorbance and carried out using an arsenic hollow-cathode lamp (GBC) at 193.7 nm. Calibration curve in the concentration range 1–20 µg l^{-1} was achieved using dilutions prepared from standard As solutions. The detection limit was 0.2 µg l^{-1} and the relative standard deviation in the range of 1–20 µg l^{-1} was ±4.0%.

2.7 Adsorption experiment

50 ml of As(V) solution of known concentration were added to 100 ml flask containing 0.1 g adsorbent and shaken well for 4 h. the suspensions were filtered and the concentration of As was found out using AAS. The amount of adsorption (qe) was calculated using the equation:

$$qe = \frac{C0 - Ce}{m} V \quad (1)$$

where C_o and C_e are the initial and equilibrium As(V) concentrations, respectively. V is the volume of the solution and m is the amount of adsorbent used. In the present work, the effects of pH, contact time, initial concentration of solute, temperature and adsorbent dose on As(V) removal process were studied. The effect of the equilibrium pH on As(V) adsorption with composite was investigated using an adsorbent dose of 0.1 g in 50 ml at As(V) concentrations of 1 and 5 mg l^{-1}. The starting solution pH was initially adjusted with 0.1 M HCl and NaOH solutions and was determined using a pH meter. Kinetic studies were carried out at pH 7.0, with an initial concentration range from 5 to 20 mg l^{-1}. Samples were withdrawn at regular intervals to show the removal percentage versus time. Isotherm experiments were performed using different initial concentrations ranging between 5 and 100 mg l^{-1} at 20, 30, 40 and 50^0C.

2.8 Desorption experiment

The most important thing in the adsorption process are the recovery of adsorbent and finding out capacity of regeneration. Desorption studies of the adsorbed As were carried out by shaking the composite in 0.1 M HCl for a period of 4 h. After equilibrium, the sorbent was filtered and washed. The adsorbed As was eluted with 50 ml of 0.1 M HCl. After mixing for 4 h, the suspension was filtered and the filtrate was analysed for As. A comparison of the value with those observed in the initial sorption step was used to compute the percentage recovery values. The sorbent sample thus regenerated was reused for adsorption. The loading and regeneration cycles were repeated four times.

3. RESULTS AND DISCUSSION:

3.1 FT-IR analysis

The FTIR spectra of CF, PCC, PCC-AE and PCC-AE/MCHI were explained in **Fig. 1**. Generally, the broad absorption bands observed at 3431 cm^{-1} were related to O-H stretching vibration of hydroxyl group and band at 2904 cm^{-1} was related to C-H stretching vibration of methyl and methylene groups (**30**). The peak at 1739 cm^{-1} was due to acetyl groups of hemicellulose and the carbonyl groups of lignin. Compared with the spectrum of CF (Fig. 2a), the intensities of absorption bands (1739 cm^{-1}) from PCC (Fig. 2b) and PCC-AE (Fig. 2c) were significantly weakened, which demonstrated that greater part of the hemicelluloses and lignin in CF had been expelled during the earlier purification steps. It is plausible that the absorption bands at 1630 cm^{-1} for CF and PCC were due to the moisture content (**31**). The absorptions at 1514 cm^{-1} and 1265 cm^{-1} were associated to the ring stretching vibration of aromatic C=C in lignin and the stretching vibration of acetyl groups of hemicellulose, respectively (**30**). The IR spectrum of PCC shows an asymmetric absorption band at 3275 cm^{-1} which is due to the hydrogen bonded O–H stretching vibration from the cellulose structure of the PCC. The absence of this band in PCC–AE indicates the participation of –OH groups due to cellulose for epoxide formation with epichlorohydrin. Additional peaks at 1450 cm^{-1} and 1131 cm^{-1} in PCC–AE indicate the presence of aliphatic CN vibration and-CH_2–$^+$NH $(CH3)_2$ type nitrogen. These observations clearly indicate the formation of chain (back bone) and the presence of -CH_2–$^+$NH $(CH3)_2$ groups in PCC–AE (**32).** The disappearance of the absorptions at 1514 cm^{-1} and 1265 cm^{-1} in the spectra of PCC and PCC-AE was also in good agreement with their low contents of hemicellulose and lignin. In addition, the C-O asymmetric stretching vibration (1164 cm^{-1}), skeletal vibration of pyranose rings (1056 cm^{-1}), and rocking vibrations of C-H (894 cm^{-1}) were corresponded to the characteristic values of cellulose (**33, 34**). The peaks at 1,160 and 1,070 cm-1 are related to the saccharide structure (**35**). The peaks at about 539 $cm^{-1}$is characteristic of the Fe3O4 phase and thus are ascribed to the stretching vibration of Fe-O bonds in the composite (**36**).

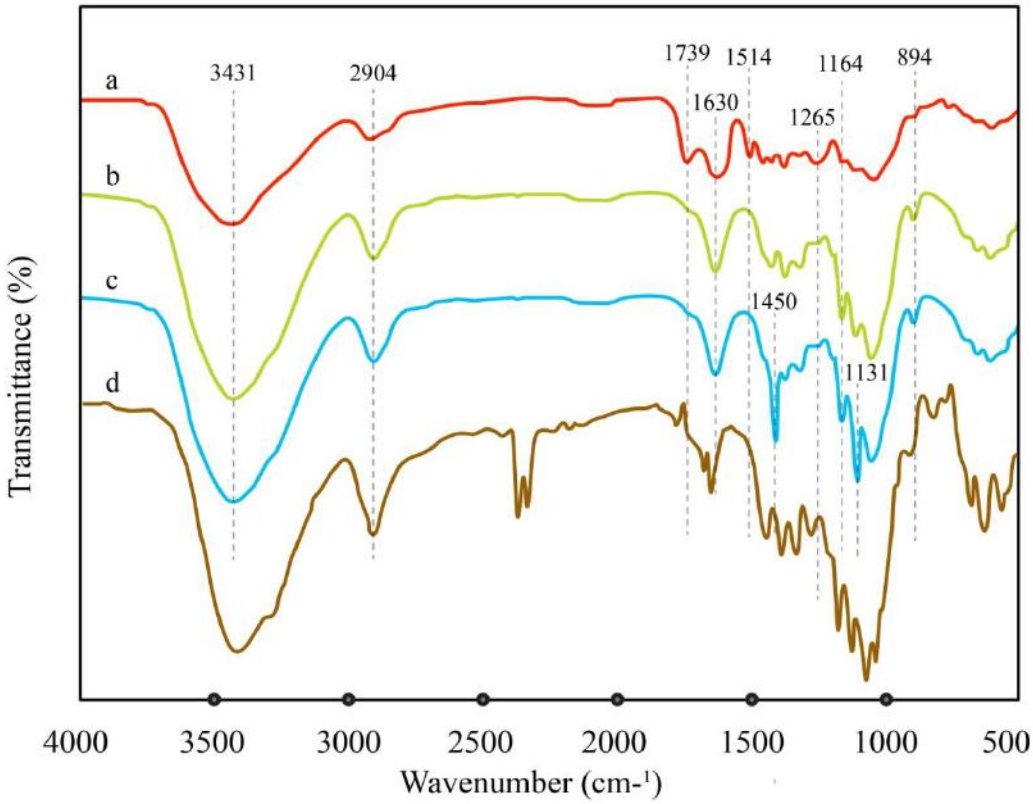

Fig.1FT-IR spectrum of (a) CF (b)PCC (c)PCC- AE (d) PCC-AE/ MCHI

3.2 XRD analysis

As appeared in **Fig. 2**, two groups of signals were demonstrated for CF (**Fig. 2c**). The left broad one locating around 16° is an overlapped signal donated by 101 plane and 101 plane of cellulose, while the relatively sharper one close to 22° with higher intensity is mainly related to 002 plane. After a variety of chemical treatments and purification steps, the peak of 002 plane was slightly shifted to~23° (**Fig. 2b**), attributed to the removal of majority of lignin and hemicellulose (**37**). Furthermore, the cellulose component in PCC still maintained the crystal structure of cellulose I (**38**), avoiding extensive structural changes resulted from chemical treatment. In the crystalline region cellulose molecules are arranged in an ordered lattice in which –OH groups are bonded by strong secondary forces.

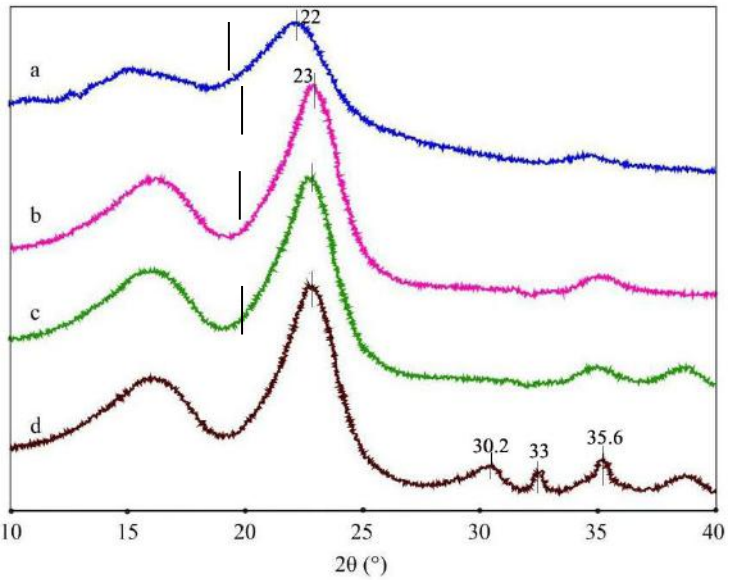

Fig.2 XRD spectrum of (a) CF (b)PCC (c)PCC- AE (d) PCC-AE/ MCHI

3.3 Effects of the individual parameter on removal efficiency

3.3.1Contact time

Estimation and improvement of contact time are of most extreme significance adsorption-based treatment framework. In this way, for the current investigation, in the 100-mL arrangement of As(v) concentration, a fixed measure of composite was included and shaken for various time spans running from 10–300 min. pH of the arrangement was kept up at 6.5 and adsorption try was performed at 25 °C. Consequences of contact time streamlining demonstrated that the rate As (V) expulsion expanded with increment in contact time until all its active site were involved and there was no more adsorption of As(V) (**Fig.3a**).

3.3.2 Adsorbent dose

Sorption try was performed at the temperature of 25 °C. The impact of adsorbent portion on As (V) adsorption is shown in **Fig.3b**. The adsorption of As (V) got improved with the expansion in adsorbent portion. As (V) adsorption onto composite indicated that adsorption got consistent above 2.5 g/L of measurement. It demonstrated that solute was utilized totally. Further increment in adsorbent portion had not indicated any generous increment in removal. This may be because of the connection of all As (V) particles on the adsorbent locales or accomplishing the equillibrium.

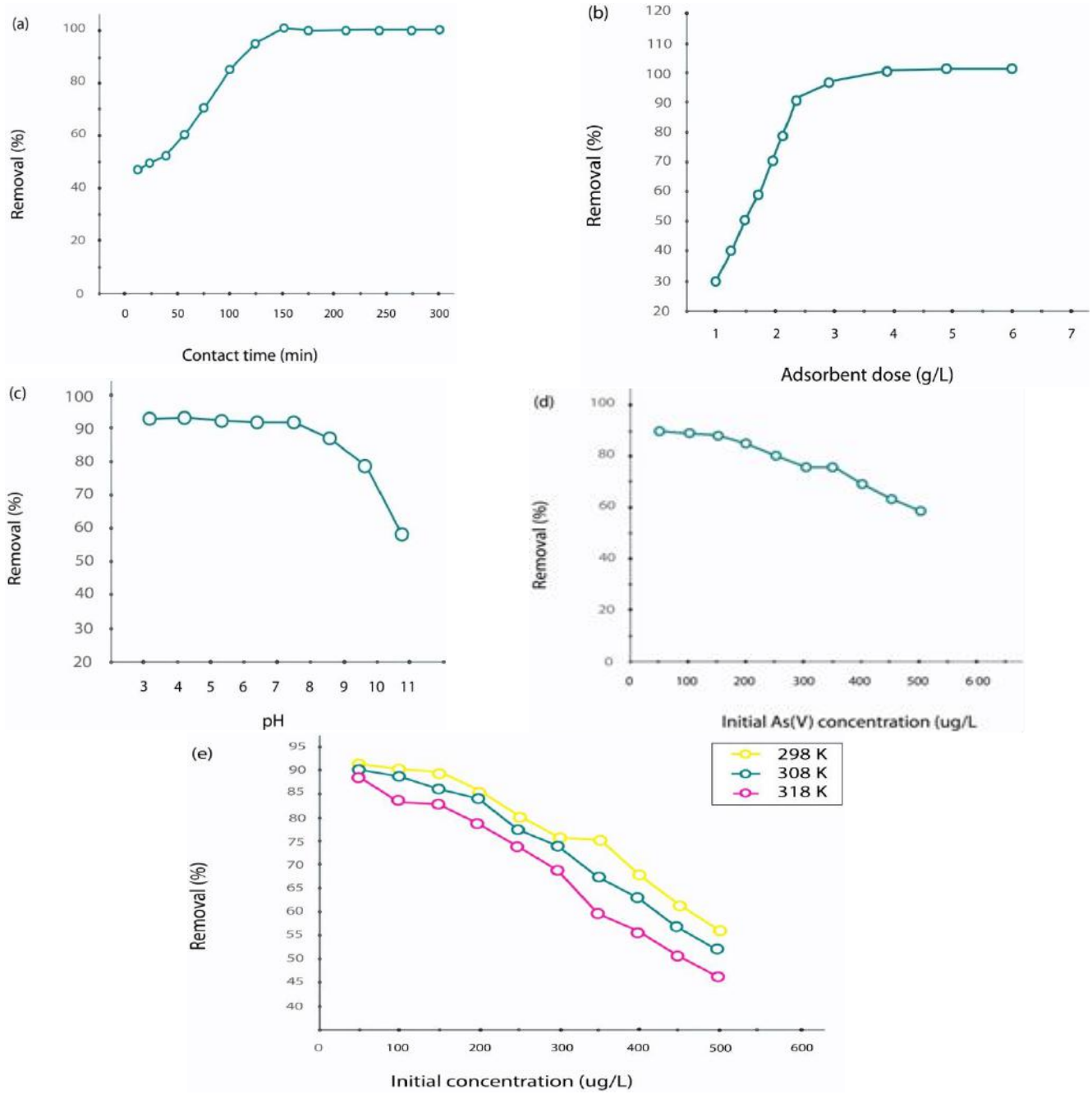

Fig.3 a- e Effects of individual parameter on As(V) removal of (a) contact time (b) adsorbent dose (c) pH (d) initial concentration and (e) temperature

3.3.3 pH

pH significantly influences the adsorbent surface charge. So, it is of prime significance to locate an appropriate and ideal pH for the productive evacuation of As (V). pH of the solution was changed from 3.5 to 10.5. Different parameters were kept equivalent to examined in past enhancement contemplates. Over 90% of expulsion was seen up to pH 7.5, yet rate As(V) evacuation diminished when pH increased above 7 (**Fig.3c**). Increment in pH made the adsorbent surface adversely charged that caused aversion between the equivalents charged species (**40**).

3.3.4 Initial As (V) concentration

Range of concentrations varying from 50 to 500 µg/L was used here. One hundred milliliters of the solution of the mentioned concentrations having pH 6.5 was made and to this, a fixed amount of composite was added. The samples were agitated for 120 min. From the experimental data, it was established that the removal efficiency depends on the concentration of arsenate. The percentage As (V) removal got decreased with rising concentration. 2.5 g/L of composite dose was found effective to bring the As (V) concentration below 10 µg/L up to the concentration of 150µg/L(**Fig.3d**). This happened due to more number of arsenate ions contending for the accessible sites for adsorption. Similarly, at higher concentrations, sites of adsorption were limited.

3.3.5 Temperature

To know the effect of temperature, experiments were executed at three different temperatures (298–318 K). From **Fig.3e**, it was perceived that adsorption kept on decreasing for all studied concentrations by changing the experimental temperature from 298 to 318 K. The removal performance was highest at 298 K. The elevated temperature of solution has been observed to be less effective for the enhancement in removal efficiency. The results preliminary reflected the exothermic nature of adsorption. With this observation, it can be hypothesized that with an increase in temperature, surface might have attained higher energy which caused the escaping of adsorbed arsenate ions into bulk solution.

3.4 Adsorption kinetics

Pseudo-first-order kinetic model(**41**) and pseudosecond- order kinetics (**42**) was applied to the experimental data. Nonlinear equations of these models are expressed by Eqs. (**2**) and (**3**).

$$q_t = qe\,(1-e^{-k_1 t}) \qquad (2)$$

$$q_t = \frac{k_2 qe^2 t}{1+k_2 q_e t} \qquad (3)$$

where k is the second-order rate constant (g mg_1 min_1), qe and qt are the amount of metal ions adsorbed at equilibrium and at time t, respectively

To measure the degree of fitness of this model with actual kinetic data, correlation coefficient (R2) values were computed. Higher R2 (>0.98) values obtained for the pseudo-second order model indicate that this model could define the experimental results in the present system. The experimental qe points and the modeled kinetic theoretical curves, for different initial concentration are illustrated in **Figure 4**. The estimated kinetic parameters are presented in **Table.1**. The pseudo-second-order kinetic model had the highest R2 than those of the pseudo-first-order models. From Fig. it can be observed that the theoretical qt values for all concentrations were very close to the experimental qt values. The reaction mechanism therefore may be partly a result of the ion exchange followed by complexation between the As(V) species and –NH+(CH3)2Cl_ groups on the PCC–AENF.

To better understand the removal mechanism of As(V) by the composite, the As(V) kinetic data were also evaluated using an intra-particle diffusion (IPD) model. The IPD is described by the Weber–Morris equation (**43**):

$$q_t = K_{id}^{0.5} + C \qquad (4)$$

Where, Kp(g mg−1 min−0.5) is the diffusion rate constant of IPD, C is a constant related to the boundary layer thickness, and t(min) is the adsorption time.

Pseudo-first order	Parameters	1 mg L−1	2 mg L−1	10 mg L−1
	qe1 (mg g−1)	1.1736	1.9342	6.3118
	k (min −1)	0.6907	1.0351	0.4661
	R2	0.9939	0.9925	0.9654
Pseudo-second	qe2 (mg/g)	1.2045	1.9615	6.5661
	K2(g mg−1 min	1.2888	1.5332	0.1239

order	−1)			
	R2	0.9942	0.9983	0.9859
Intra-particle model	Kp	2.4762	0.8590	0.5063
	C	1.1800	0.1310	0.0336
	R2	0.9771	0.9064	0.9808

Table.1 Kinetic fitting parameters for As(V) Adsorption onto the composite.

According to the IPD model, if the plot of qt versus t0.5 is linear and passes through the origin, the IPD is the rate–limiting factor for adsorption. However, if the IPD plot exhibits multilinearity, then both IPD and boundary diffusion contribute to the adsorption process [32].

Fig. 5 shows the plot of qt versus t0.5 for different initial As (V) concentrations at T = 25 °C.

The plot exhibits multi linearity, indicating that IPD does not govern the As (V) adsorption process. The first step is a steep slope and it can be associated with the surface adsorption of the As (V) onto the most readily available adsorbing sites on the composites (**44**). The second step is relatively moderate adsorption and the third slow adsorption step is attributed to the stereo-hindrance effect caused by the adsorbed As(V) and the decrease of vacant and easily accessible adsorption sites on PCC AENF.

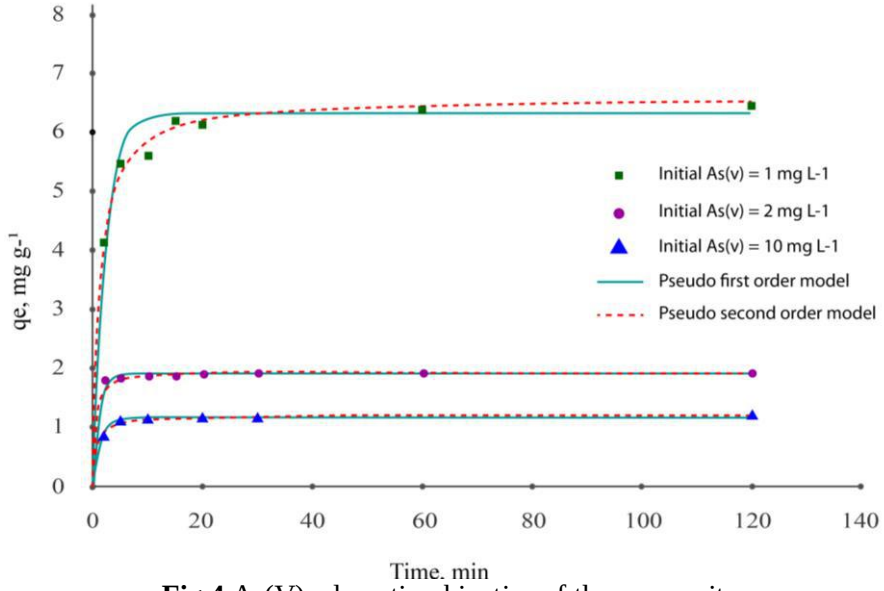

Fig.4 As(V) adsorption kinetics of the composite

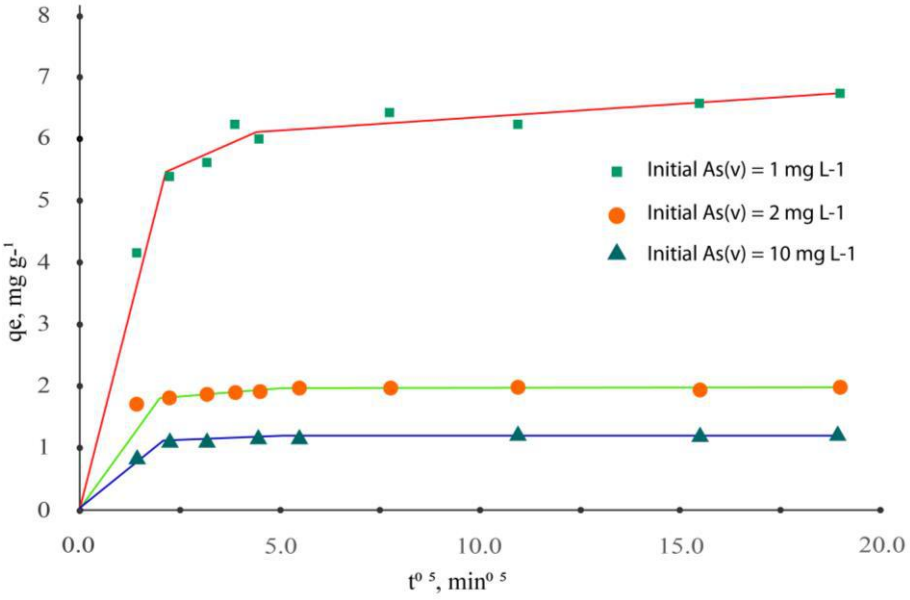

Fig.5 Intraparticle diffusion model of As(V) adsoprtion by composite

3.5 Adsorption isotherm

Adsorption isotherm studies are of fundamental importance in determining the adsorption capacity of As(V) onto composite and to diagnose the nature of adsorption (**Fig. 7).**The As (V) adsorption isotherms concentrations at four different temperatures, 25°C, 35°C, 45°C, and 55°C are plotted here. It can be seen that all the adsorption isotherms exhibit an L-shape, which corresponds to the classification of Giles (**45**). Two isotherm models; Langmuir and Freundlich, were used to evaluate the adsorption equilibrium data.

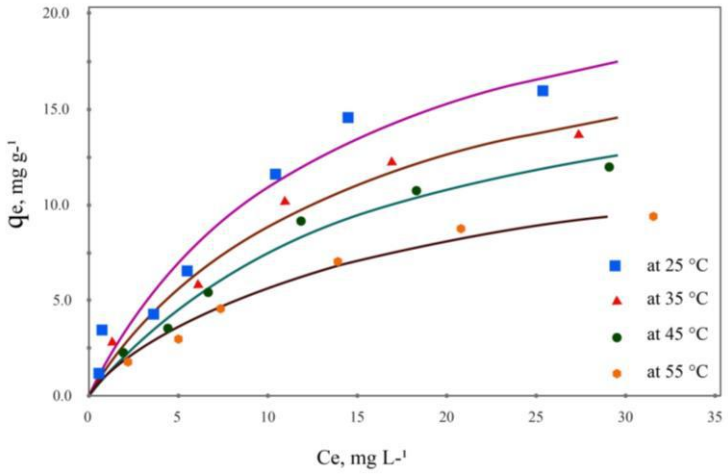

Fig.6 As(V) adsorption isotherms of the composite.

In the Langmuir model the adsorption is assumed to be monolayer on a homogeneous surface. The Langmuir model is described by:

$$q_e = \frac{Q^0 bC_e}{1 + bC_e} \quad (5)$$

Where, qe(mg g−1) is the adsorption capacity at equilibrium, Ce(mg L−1) is the concentration of As(V) in solution at the equilibrium, qm(mg g−1) is the monolayer adsorption capacity of Langmuir, and b(L mg−1) is an equilibrium constant (**46**). The Freundlich model is empirical and assumes the adsorption to be multilayer on a heterogeneous surface with a non-uniform distribution (**47**) and is described as:

$$qe = KfCe^{1/N} \quad (6)$$

Where, qe and Ce are the same as the Langmuir equation, Kf (mg g−1) is the adsorption capacity of Freundlich and n is the Freundlich adsorption intensity. The Langmuir model provided the best fit (Figure 8) as it had the highest R2 and the lowest standard errors for its coefficients suggesting that it is more suitable to characterize the adsorption process. The Langmuir maximum adsorption capacity (qm) for As(V) removal by modified-CNF is 25.5 mg g−1. The Langmuir maximum uptake capacity was found higher than some of the adsorbents cited in the literature for As(V) removal (Table.2). Fig.8 shows that the As(V) removal by modified-CNF is pH-dependent. Between pH 4 and 8, more than 97% of As(V) was removed and the removal capacity was relatively constant at this pH range. Maximum uptake was obtained at pH 4. Similar behavior of As(V) adsorption was also reported in the literature (**48**). At pH< 4, As(V) removal was about 88% and at pH> 8 the % As(V) removal decreased significantly to 49%.

	Parameters	25 °C	35 °C	45 °C	55 °C
Langmuir	qm (mg g−1)	25.498	21.677	19.023	14.714
	b(L mg−1)	0.075	0.069	0.066	0.062
	R2	0.978	0.988	0.992	0.995
Freundlich	Kf (mg g−1)	2.659	2.015	1.672	1.258
	1/n	0.581	0.605	0.612	0.609
	R2	0.970	0.975	0.975	0.979

Table 2. Langmuir and Freundlich isotherm parameters for the adsorption of As(V) onto the composite

3.6 Thermodynamic study

The thermodynamic parameters including Gibbs free energy change (ΔG°, kJ mol−1), enthalpy change (ΔH°, kJ mol−1), and entropy change (ΔS°, J mol−1 K−1) were determined from the experimental data. These parameters were calculated using the following equations [**49, 50**]:

$$\Delta G^{\circ} = -RT\ln Kd \quad (7)$$

$$\ln Kd = (\Delta S^{\circ}/R) - (\Delta H^{\circ}/RT) \quad (8)$$

Where, R is the universal gas constant (8.314 J K−1 mol−1), T(Kelvin) is the absolute temperature, and Kd is the equilibrium constant. **Table 3** summarizes the values of ΔH°, ΔS°, and ΔG°. The negative values of ΔH° indicate that the adsorption process is exothermic, while negative values of ΔG° indicate that the adsorption is spontaneous (**51, 52**). The positive values of ΔS° could be due to the randomness increase at the solid/liquid interface during the adsorption process.

Temperature (°C)	Kd	ΔG°(kJ mol-1)	ΔS° (J moll·K-1)	ΔH° (kJ mol-1)
25	10359.25	-22.92	60.35	-4.91
35	9584.09	-23.49		
45	9101.49	-24.11		
55	8621.25	-24.72		

Table.3 Thermodynamic parameters of As(V) adsorption onto the composite.

3.7 Reusability

The reuse of the adsorbent was tried by utilizing a similar adsorbent in three back to back cycles and a NaCl convergence of 0.05 M toward the finish of each cycle. The reuse results demonstrated that the adsorption limit of the adsorbent diminished from cycle 4. Be that as it may, significantly after three sequential cycles, the adsorbent moderately held high limit with respect to As (V) removal.

4. CONCLUSION:

The present study clearly shows that the dimethyl amino hydroxyl propyl derivative of the epichlorohydrin cross linked coconut coir pith in the anion exchanger form (CP–AE), is an effective adsorbent for the removal of As(V) from aqueous solutions. Sorption of As(V) is pH-dependent and the best results are obtained at pH range 6.0–8.0. Kinetic and equilibrium studies were compiled for the adsorption of As(V) from aqueous solution onto CP– AE in the concentration range 5–100 mg l_1. The kinetics of As(V) can be described by the psuedo-second-order model. The equilibrium adsorption isotherm data were fit by the Langmuir model. The process is exothermic in nature. Quantitative removal of As(V) from simulated groundwater confirmed the validity of the results in batch wise studies. The spent adsorbent can be regenerated and reused by 0.1 N HCl.

REFERENCES:

1. C.-S. Fan, S.-C. Tseng, K.-C. Li and C.-H. Hou, Electroremoval of arsenic(III) and arsenic(V) from aqueous solutions by capacitive deionization, J. Hazard. Mater., 2016, 312, 208–215.
2. P. Pal, Groundwater Arsenic Remediation: Treatment Technology and Scale UP, Elsevier Science, 2015.
3. Roghani, M.; Nakhli, S.A.A.; Aghajani, M.; Rostami, M.H.; Borghei, S.M. Adsorption and oxidation study on arsenite removal from aqueous solutions by polyaniline/polyvinyl alcohol composite. J. Water Process Eng. 2016, 14, 101–107.
4. Uppal, H.; Hemlata; Tawale, J.; Singh, N. Zinc peroxide functionalized synthetic graphite: An economical and efficient adsorbent for adsorption of arsenic (III) and (V). J. Environ. Chem. Eng. 2016, 4, 2964–2975.
5. Hafeznezami, S.; Zimmer-Faust, A.G.; Jun, D.; Rugh, M.B.; Haro, H.L.; Park, A.; Suh, J.; Najm, T.; Reynolds,M.D.; Davis, J.A.; et al. Remediation of groundwater contaminated with arsenic through enhanced natural attenuation: Batch and column studies. Water Res. 2017, 122, 545–556
6. L. Fang, X. Y. Min, R. F. Kang, et al., Sci. Total Environ., 2018, 639, 110–117.
7. J. G. Hering, I. A. Katsoyiannis, G. A. Theoduloz, et al., J. Environ. Eng., 2017, 143, 117–122.
8. Chatterjee, S.; De, S. Adsorptive removal of arsenic from groundwater using chemically treated iron ore slime incorporated mixed matrix hollow fiber membrane. Sep. Purif. Technol. 2017, 179, 357–368.
9. M. A. Hoque, W. G. Burgess and K. M. Ahmed, Hydrol. Processes, 2017, 31, 2095–2109.
10. M. Monrad, A. K. Ersbøll, M. Sørensen, et al., Environ. Res., 2017, 154, 318–324.
11. T. G. Kazi, K. D. Brahman, J. A. Baig, et al., J. Hazard. Mater., 2018, 357, 159–167.
12. M. R. Awual, M. Shenashen, T. Yaita, et al., Water Res., 2012, 46, 5541–5550.
13. Saha, S.; Sarkar, P. Arsenic remediation from drinking water by synthesized nano-alumina dispersed in chitosan-grafted polyacrylamide. J. Hazard. Mater. 2012, 227–228, 68–78.

14. Siddiqui, S.I.; Chaudhry, S.A. Iron oxide and its modified forms as an adsorbent for arsenic removal: A comprehensive recent advancement. Process Saf. Environ. Prot. 2017, 111, 592–626.
15. Pintor AM, Vieira BR, Santos SC, Boaventura RA, Botelho CM (2018) Arsenate and arsenite adsorption onto iron-coated cork granulates. Sci Total Environ 642:1075–1089
16.Montero JIZ,Monteiro AS, Gontijo ES, Bueno CC, de MoraesMA, Rosa AH (2018) High efficiency removal of As (III) from waters using a new and friendly adsorbent based on sugarcane bagasse and corncob husk Fe-coated biochars. Ecotoxicol Environ Saf 162:616–624
17 A.W. Carpenter, C.F. De Lannoy, M.R. Wiesner, Cellulose nanomaterials in water treatment technologies, Environ. Sci. Technol. 49 (2015) 5277–5287.
18. M. Rahim and M. R. H. M. Haris, J. Radiat. Res. Appl. Sci., 2015, 8, 255–263.
19. R. Kumar, R. K. Sharma and A. P. Singh, J. Mol. Liq., 2017, 232, 62–93.
20. K. Singh, T.J.M. Sinha, S. Srivastava, Functionalized nanocrystalline cellulose: Smart biosorbent for decontamination of arsenic, Int. J. Miner. Process. 139 (2015) 51–63.
21. K. Singh, J.K. Arora, T.J.M. Sinha, S. Srivastava, Functionalization of nanocrystalline cellulose for decontamination of Cr(III) and Cr(VI) from aqueous system: Computational modeling approach, Clean Technol. Environ. Policy. 16 (2014) 1179–1191.
22. G. Annadurai, R.S. Juang, D.J. Lee, Use of cellulose-based wastes for adsorption of dyes from aqueous solutions, J. Hazard. Mater. 92 (2002) 263–274
23. G.L. Dotto, E.C. Lima, L.A.A. Pinto, Biosorption of food dyes onto Spirulina platensis nanoparticles: Equilibrium isotherm and thermodynamic analysis, Bioresour. Technol. 103 (2012) 123–130.
24. R. Wang, S. Guan, A. Sato, X. Wang, Z. Wang, R. Yang, B.S. Hsiao, B. Chu, Nanofibrous microfiltration membranes capable of removing bacteria, viruses and heavy metal ions, J. Memb. Sci. 446 (2013) 376–382.
25. Orlando, U.S., Baes, A.U., Nishigima, W., Okada, M., 2002. Preparation of agricultural residue anion exchangers and its nitrate maximum adsorption capacity. Chemosphere 48, 1041–1046.
26. A. Gupta, M. Yunus and N. Sankararamakrishnan, Ind. Eng. Chem. Res., 2013, 52, 2066–2072.
27. Sun, X., Sun, R., Su, Y., & Sun, J. (2004). Comparative study of crude and purified cellulose from wheat straw. Journal of Agricultural and Food Chemistry, 52, 839–847.
28. G.Z. Kyzas, E.A. Deliyanni, N. K. Lazaridis, Magnetic modification of microporous carbon for dye adsorption, Journal of Colloid and Interface Science, 430 (2014), 166–173.
29. APHA, AWWA, WEF, 1992. Standard Methods for the Examination of Water and Wastewater, 18th ed. American Public Health Association, Washington, DC.
30.Uma Maheswari, C., Obi Reddy, K., Muzenda, E., Guduri, B. R., & Varada Rajulu, A. (2012). Extraction and characterization of cellulose microfibrils from agricultural residue – Cocos nucifera L. Biomass and Bioenergy, 46, 555–563.
31.Reddy, K. O., Maheswari, C. U., Dhlamini, M. S., Mothudi, B. M., Kommula, V. P., Zhang, J., et al. (2018). Extraction and characterization of cellulose single fibers from native African napier grass. Carbohydrate Polymers, 188, 85–91.
32. Namasivayam, C., Holl, W.H., 2005. Quaternised biomass as an anion exchanger for the removal of nitrate and other anions from water. J. Chem. Technol. Biotechnol. 80, 164–168.
33. Pappas, C., Tarantilis, P. A., Daliani, I., Mavromoustakos, T., & Polissiou, M. (2002). Comparison of classical and ultrasound-assisted isolation procedures of cellulose from kenaf (Hibiscus cannabinus L.) and eucalyptus (Eucalyptus rodustrus Sm.). Ultrasonics Sonochemistry, 9, 19–23.
34. Sun, X., Sun, R., Su, Y., & Sun, J. (2004). Comparative study of crude and purified cellulose from wheat straw. Journal of Agricultural and Food Chemistry, 52, 839–847.
35.de Mesquita JP, Donnici CL, Pereira FV (2010) Biobased nanocomposites from layer-by-layer assembly of cellulose nanowhiskers with chitosan. Biomacromolecules 11:473– 480
36. C. Yang, C. Wang, K. Huang, C. Kung, Y. Chang, J. Shaw, Microfluidic one-step synthesis of Fe3O4- chitosan composite particles and their applications, International Journal of Pharmaceutics, 463 (2014), 155– 160
37. Nazir, M. S., Wahjoedi, B. A., Yussof, A. W., & Abdullah, M. A. (2013). Eco-friendly extraction and characterization of cellulose from oil palm empty fruit bunches. Bioresources, 8, 2161–2172.
38.Flauzino Neto, W. P., Silvério, H. A., Dantas, N. O., & Pasquini, D. (2013). Extraction and characterization of cellulose nanocrystals from agro-industrial residue-soy hulls. Industrial Crops and Products, 42, 480–488.
39. Abdul Rahman, N. H., Chieng, B. W., Ibrahim, N. A., & Abdul Rahman, N. (2017). Extraction and characterization of cellulose nanocrystals from tea leaf waste fibers. Polymers, 9(11), 588

40. Prabhakar R, Samadder SR (2018) Low cost and easy synthesis of aluminium oxide nanoparticles for arsenite removal from groundwater: a complete batch study. J Mol Liq 250:192–201
41.Lagergren SK (1898) About the theory of so-called adsorption of soluble substances. Sven Vetenskapsakad Handingarl 24:1–39
42.Ho YS (1995) Absorption of heavy metals from waste streams by peat (Doctoral dissertation, University of Birmingham)
43. J. Lin, L. Wang, Comparison between linear and non-linear forms of pseudo-firstorder
and pseudo-second-order adsorption kinetic models for the removal of methylene blue
by activated carbon, Front. Environ. Sci. Eng. China. 3 (2009) 320–324.
44. Y. Yoon, M. Zheng, Y.T. Ahn, W.K. Park, W.S. Yang, J.W. Kang, Synthesis of magnetite/non-oxidative graphene composites and their application for arsenic removal, Sep. Purif. Technol. 178 (2017) 40–48.
45. Giles, C.H., McEwan, T.H., Nakhwa, S.N., Smith, D., 1960. Studies in adsorption. Part II. A system of classification of solution adsorption isotherm. J. Chem. Soc. 4, 3973–3993.
46. L.L. Min, L. Bin Zhong, Y.M. Zheng, Q. Liu, Z.H. Yuan, L.M. Yang, Functionalized chitosan electrospun nanofiber for effective removal of trace arsenate from water, Sci. Rep. 6 (2016). doi:10.1038/srep32480.
47. C.G. Lee, P.J.J. Alvarez, A. Nam, S.J. Park, T. Do, U.S. Choi, S.H. Lee, Arsenic(V) removal using an amine-doped acrylic ion exchange fiber: Kinetic, equilibrium, and regeneration studies, J. Hazard. Mater. 325 (2017) 223–229.
48. Y. Tian, M. Wu, R. Liu, D. Wang, X. Lin, W. Liu, L. Ma, Y. Li, Y. Huang,
Modified native cellulose fibers-A novel efficient adsorbent for both fluoride and arsenic, J.
Hazard. Mater. 185 (2011) 93–100. doi:10.1016/j.jhazmat.2010.09.001
49. R. Han, Y. Wang, P. Han, J. Shi, J. Yang, Y. Lu, Removal of methylene blue from aqueous solution by chaff in batch mode, Journal of Hazardous Materials. 137 (2006) 550–557
50. J. Ray, S. Jana, T. Tripathy, Synthesis of dipolar grafted hydroxyethyl cellulose and its application for the removal of phosphate ion from aqueous medium by adsorption, International Journal of Biological Macromolecules. 109 (2018) 492–506.
51. Y. Liu, Y.-J. Liu, Biosorption isotherms, kinetics and thermodynamics, Separation and Purification Technology. 61 (2008) 229–242. doi:10.1016/j.seppur.2007.10.002.
52. Y. Liu, H. Xu, Equilibrium, thermodynamics and mechanisms of Ni2 biosorption
by aerobic granules, Biochemical Engineering Journal. 35 (2007) 174–182.